

Open Research Online

The Open University's repository of research publications and other research outputs

Oxygen diffusion in $\text{Sr}_{0.75}\text{Y}_{0.25}\text{CoO}_{2.625}$: a molecular dynamics study

Journal Item

How to cite:

Rupasov, D.; Chroneos, A.; Parfitt, D.; Kilner, J. A.; Grimes, R. W.; Istomin, S. Ya. and Antipov, E. V. (2009). Oxygen diffusion in $\text{Sr}_{0.75}\text{Y}_{0.25}\text{CoO}_{2.625}$: a molecular dynamics study. *Physical Review B (Condensed Matter and Material Physics)*, 79(17) p. 172102.

For guidance on citations see [FAQs](#).

© 2009 The American Physical Society

Version: Version of Record

Link(s) to article on publisher's website:

<http://dx.doi.org/doi:10.1103/PhysRevB.79.172102>

<http://prb.aps.org/abstract/PRB/v79/i17/e172102>

Copyright and Moral Rights for the articles on this site are retained by the individual authors and/or other copyright owners. For more information on Open Research Online's data [policy](#) on reuse of materials please consult the policies page.

oro.open.ac.uk

Oxygen diffusion in $\text{Sr}_{0.75}\text{Y}_{0.25}\text{CoO}_{2.625}$: A molecular dynamics study

D. Rupasov,^{1,2} A. Chroneos,^{2,*} D. Parfitt,² J. A. Kilner,² R. W. Grimes,² S. Ya. Istomin,³ and E. V. Antipov³

¹Department of Materials Science, Moscow State University, 119991 Moscow, Russia

²Department of Materials, Imperial College London, London SW7 2AZ, United Kingdom

³Department of Chemistry, Moscow State University, 119991 Moscow, Russia

(Received 25 March 2009; published 12 May 2009)

Oxygen diffusion in $\text{Sr}_{0.75}\text{Y}_{0.25}\text{CoO}_{2.625}$ is investigated using molecular dynamics simulations in conjunction with an established set of Born model potentials. We predict an activation energy of diffusion for 1.56 eV in the temperature range of 1000–1400 K. We observe extensive disordering of the oxygen ions over a subset of lattice sites. Furthermore, oxygen ion diffusion both in the a - b plane and along the c axis requires the same set of rate-limiting ion hops. It is predicted that oxygen transport in $\text{Sr}_{0.75}\text{Y}_{0.25}\text{CoO}_{2.625}$ is therefore isotropic.

DOI: 10.1103/PhysRevB.79.172102

PACS number(s): 66.30.Lw, 82.47.Ed, 61.43.Bn

New solid-oxide fuel cell (SOFC) electrode materials must show improved performance at lower temperatures and resistance to degradation during operation. In that respect perovskite-related materials such as cobalt-based oxides are important candidate cathode materials for the next-generation SOFC because of their catalytic properties in addition to their high electronic and oxide conductivity. The structure and oxygen transport of the $\text{Sr}_{1-x}\text{Ln}_x\text{CoO}_{3-\delta}$ (Ln = rare-earth cations) complex cobalt oxides has been previously studied.^{1–8} Cobalt oxides such as $\text{Sr}_{1-x}\text{Y}_x\text{CoO}_{3-\delta}$ are also potentially important as they can be used in dense membranes to separate oxygen from gas mixtures and because they exhibit a metal-insulator transition, a spin-state transition, and ferromagnetism.^{9–15}

A detailed knowledge of crystal structure and stoichiometry is essential in order to understand the mechanism of ionic diffusion. It was determined by Istomin *et al.*,¹⁴ using synchrotron x-ray and neutron powder diffractions, that $\text{Sr}_{0.7}\text{Y}_{0.3}\text{CoO}_{2.62}$ exhibits the tetragonal symmetry (space group $I4/mmm$, No. 139). In this crystal structure the layers of CoO_6 octahedra alternate with oxygen-deficient layers that consist of O3, O4, and Co1 sites (see Fig. 1). Additionally, the O4 site was determined to have a partial occupancy of $\frac{1}{4}$, with only one of the four adjacent position of O4 being occupied.

Atomistic simulations can provide detailed information concerning the intrinsic disorder processes and diffusion mechanisms of inorganic materials.^{16–21} The primary aim of the present study is to predict the oxygen-diffusion mechanism in $\text{Sr}_{0.75}\text{Y}_{0.25}\text{CoO}_{2.625}$ (also known as the 314 phase) using classical molecular dynamics (MD) simulations.

MD simulations are essentially the iterative solution of Newton's equations of motion for an ensemble of particles. MD simulations require a potential-energy function that describes the forces between the ions. Here the classical Born-type description of the ionic crystal lattice is used.²² In this, interactions between ions i and j are described by a long-range Coulombic (summed using Ewald's method²³) and a short-range parametrized Buckingham pair potential,²⁴ the latter summed to the cutoff value of 10.5 Å. The lattice energy is given by

$$E_L = \sum_{j>i} \sum \left[\frac{q_i q_j}{4\pi\epsilon_0 r_{ij}} + A_{ij} \exp\left(\frac{-r_{ij}}{\rho_{ij}}\right) - \left(\frac{C_{ij}}{r_{ij}^6}\right) \right], \quad (1)$$

where r_{ij} is the interionic separation, q_i is the charge of ion i , ϵ_0 is the permittivity of free space, and A_{ij} , ρ_{ij} , and C_{ij} are the short-range parameters of the Buckingham pair potential (see Table I). The short-range parameters used here were reported previously,^{25–28} and their efficacy was established by comparing the predictions to experimental lattice properties.^{29–31} For $\text{Sr}_{0.75}\text{Y}_{0.25}\text{CoO}_{2.625}$ the predicted unit-cell volume is within 0.7% of the experimental volume.¹⁴

The initial configurations for the present simulations are based on the structure of $\text{Sr}_{0.75}\text{Y}_{0.25}\text{CoO}_{2.625}$ determined by Istomin *et al.*¹⁴ The infinite periodic crystal lattice is constructed from a supercell of $6 \times 6 \times 3$ unit cells (containing 7992 ions), tessellated throughout space through the use of periodic boundary conditions, which are defined by the crystallographic lattice vectors. Newton's equations of motion were integrated using the velocity Verlet algorithm.³² Ions were assigned a Gaussian distribution of velocities and with

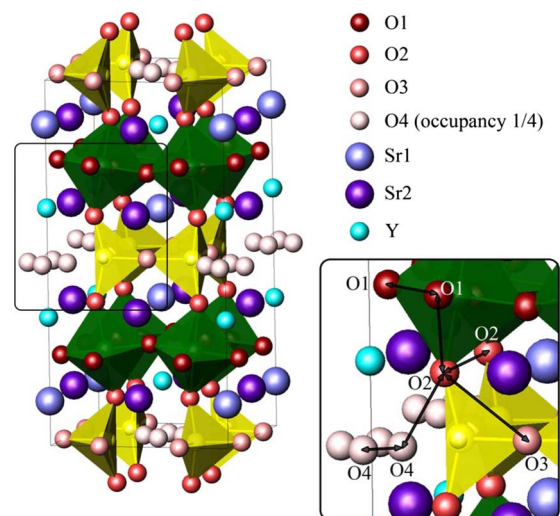


FIG. 1. (Color online) In the crystal structure of $\text{Sr}_{0.7}\text{Y}_{0.3}\text{CoO}_{2.62}$ the CoO_6 octahedra layers alternate with oxygen-deficient layers that consist of O3, O4 (occupancy factor of $\frac{1}{4}$), and Co1 atoms.

TABLE I. Buckingham interionic potential parameters [see Eq. (1)].

Interaction	A_{ij} (eV)	ρ_{ij} (Å)	C_{ij} (eV Å ⁶)	Reference
O ²⁻ -O ²⁻	9547.96	0.2192	32.0	25
Sr ²⁺ -O ²⁻	682.17	0.3945	0.0	26
Y ³⁺ -O ²⁻	1766.40	0.33849	19.43	27
Co ³⁺ -O ²⁻	1226.31	0.3087	0.0	28

iterative velocity scaling, a stable temperature was achieved. The system was equilibrated for 5000 time steps (~ 5 ps) before carrying out the production runs that were used in the analysis. We used the variable time step option as implemented in the DLPOLY code for efficient sampling of the dynamic behavior.^{33,34} Typical time steps are on the order of 1 fs, and up to 250 000 time steps were used to investigate the diffusion processes in the temperature range of 500–1500 K. Simulations were run in the constant number of atoms-pressure-temperature (*NPT*) ensemble to predict the equilibrium lattice parameters and the constant number of atoms-volume-temperature (*NVT*) ensemble to predict the diffusion properties. The temperature, and where necessary the pressure, was corrected with the use of the Nosé-Hoover thermostat.^{35,36}

In the present MD simulations ionic transport was determined by monitoring the evolution of the mean-square displacement (MSD) of ions as a function of time for a range of defect temperatures. Extensive simulation times were used to consider a sufficient number of diffusion events for effective statistical sampling. The MSD of an ion i at a position $r_i(t)$ at time t with respect to its initial position $r_i(0)$ is defined by

$$\langle r_i^2(t) \rangle = \frac{1}{N} \sum_{i=1}^N [r_i(t) - r_i(0)]^2, \quad (2)$$

where N is the total number of ions in the system. All the cations considered (i.e., Sr, Y, and Co) oscillate around their equilibrium positions; above 900 K, however, oxygen ions demonstrate an increasing MSD with time. This in turn indicates that oxygen self-diffusion is significant at high temperatures, whereas the cation self-diffusion is insignificant on the time scales considered.

The oxygen-diffusion coefficient D can be obtained directly from the slopes of MSD for a range of temperatures using³⁷

$$\langle |r_i(t) - r_i(0)|^2 \rangle = 6Dt + B, \quad (3)$$

where $|r_i(t) - r_i(0)|$ is the displacement of an ion from its initial position and B is an atomic displacement parameter that can be attributed to thermal vibrations. Here we predict values for D over the range of temperatures 1000–1400 K and these are presented in the Arrhenius plot of Fig. 2. We find that over this temperature range, oxygen transport in Sr_{0.75}Y_{0.25}CoO_{2.625} can be described by the Arrhenius relation with an activation energy of 1.56 eV. At lower temperatures we would expect a lower frequency of events that

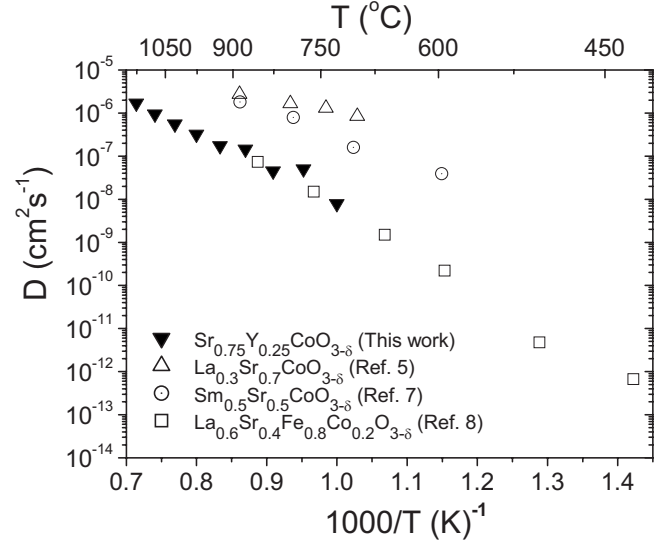


FIG. 2. Arrhenius plot of the calculated oxygen diffusivity in Sr_{0.75}Y_{0.25}CoO_{2.625}. The present results are compared with the experimental results of van Doorn *et al.* (Ref. 5), Fullarton *et al.* (Ref. 7), and Benson *et al.* (Ref. 8).

would necessitate simulation times that are beyond our computational resources. The energy required for an oxygen ion to migrate from an O4 site to an adjacent unoccupied O4 site is very small, about 0.1 eV. These events, however, do not lead to a net diffusion of the oxygen atoms.

Figure 2 compares the present predicted values of oxygen-diffusion coefficient with previous experimental results from studies of related cobalt oxides such as La_{0.3}Sr_{0.7}CoO_{3-δ} (van Doorn *et al.*⁵), Sm_{0.5}Sr_{0.5}CoO_{3-δ} (Fullarton *et al.*⁷), and La_{0.6}Sr_{0.4}Fe_{0.8}Co_{0.2}O_{3-δ} (Benson *et al.*⁸). Interestingly, in spite of their compositional differences, these observed diffusivities are in good agreement with the present predicted diffusivities.

A significant advantage of MD over other techniques is that it can reveal the transport mechanisms of atoms by the direct observation of ion trajectories and hence reveal any significant anisotropy. The calculated oxygen MSD in the a (or b as they are symmetrically equivalent) and c directions are surprisingly almost equal and therefore the transport of oxygen is predicted to be isotropic. Figures 3(a) and 3(b) represent an example of the oxygen-diffusion pathways on two (001) plane slices ($z=0$ and $z=0.25$) in Sr_{0.75}Y_{0.25}CoO_{2.625} at 1300 K.

At temperatures above 700 K, the oxygen ion at the O4 sites hops around the four equivalent sites [see Fig. 3(a)], in excellent agreement with previous experimental (neutron) studies,^{14,15} as a result of the low activation energy for this process. At higher temperatures the thermal ellipsoid describing the O2 site becomes increasingly distorted along the (111) direction toward the neighboring partially occupied O4 sites [see Fig. 3(c)]. Additionally, at temperatures over 1000 K there is significant intermingling of the oxygen ions from O2 and O4 sites [see Fig. 3(c)]. Hopping analysis reveals the possibility of a distinct O5 site (0.35, 0.35, 0.07) at high temperatures near O2 and this will be investigated further.

The disorder between the O2 and O4 sites does not pro-

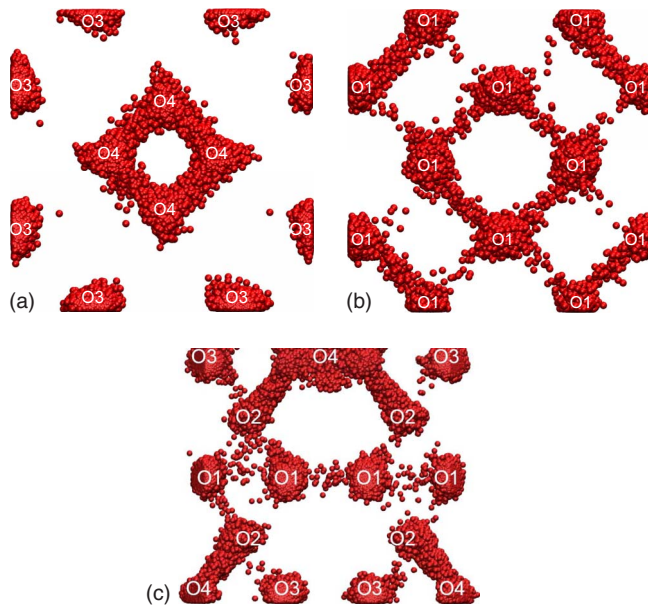


FIG. 3. (Color online) Calculated oxygen-density profiles in $\text{Sr}_{0.75}\text{Y}_{0.25}\text{CoO}_{2.625}$ at 1300 K along (a) the (001) plane at $z=0$, (b) the (001) plane at $z=0.25$, and (c) the (110) plane through the origin (half the unit cell), showing the diffusion pathways.

vide the extended network of interconnected sites necessary for bulk oxygen diffusion. It does, however, provide a supply of oxygen vacancies at the O2 site. The dominant diffusion mechanism is the movement of these vacancies to the Co-O1/O2 octahedra, which leads to migration in the a - b plane through interconnected O1 sites at $z=0.25$ and 0.75 [see Fig. 3(b)] and migration along the c axis through the O2-O1-O2 pathway (see inset in Fig. 1) and then into the highly disordered O4/O2 sites. As the barrier to exchange across the O4/O2 sites is very low, we suggest that transport along the c axis and in the a - b plane will be rate limited by the move-

ment of oxygen vacancies around the Co-O1/O2 octahedra (note that analysis of oxygen-density profiles reveals that O2-O1 hops occur at almost the same rate as O1-O1 hops), leading to a migration probability and therefore diffusivity that is isotropic. Finally, it is predicted that the O3 ions do not effectively participate in the dominant oxygen-diffusion mechanism, although very limited exchange of O3 with O4 is observed at very high temperatures.

In the present study we have examined the migration of oxygen ions at elevated temperatures. The imposition of NVT conditions on the calculations is a necessary restriction but it does imply that the stoichiometry of the material does not change with temperature. This is an approximation, as in a thermogravimetric study of the related compound $\text{Sr}_{0.7}\text{Y}_{0.3}\text{CoO}_{2.62}$ it was observed that there is significant oxygen loss at around 673 K.¹⁴ The introduction of oxygen vacancies is expected to lead to an increase in the diffusivity from the already significant levels calculated in this study, provided no extra defect interactions are introduced by the extra vacancies and the change in oxidation state of the Co cations.

In summary, molecular dynamics simulations predict that oxygen transport in $\text{Sr}_{0.75}\text{Y}_{0.25}\text{CoO}_{2.625}$ is isotropic with an activation energy of 1.56 eV in the temperature range of 1000–1400 K. The diffusion mechanism consists of O2 atoms moving to the partially occupied O4 sites creating vacancies at O2 sites. These vacancies move to the Co-O1/O2 octahedra (a - b -plane migration) and along the O2-O1-O2 pathway (c -axis migration). The effect of oxygen stoichiometry on the diffusion mechanism is currently under investigation.

The authors thank Andrey Berenov for useful discussions. The work was supported by UKERC from NERC TSEC program under Grant No. NE/C513169/1. Computing resources were provided by the HPC facility of Imperial College London.

*alexander.chroneos@imperial.ac.uk

¹J. Sunstrom, K. V. Ramanujachary, and M. Greenblatt, *J. Solid State Chem.* **139**, 388 (1998).

²R. H. E. van Doorn and A. J. Burggraaf, *Solid State Ionics* **128**, 65 (2000).

³S. Ya. Istomin, O. A. Drozhzhin, G. Svensson, and E. V. Antipov, *Solid State Sci.* **6**, 539 (2004).

⁴S. Carter, A. Selcuk, R. J. Carter, J. Kajda, J. A. Kilner, and B. C. H. Steele, *Solid State Ionics* **53-56**, 597 (1992).

⁵R. H. E. van Doorn, I. C. Fullarton, R. A. de Souza, J. A. Kilner, H. J. M. Bouwmeester, and A. J. Burggraaf, *Solid State Ionics* **96**, 1 (1997).

⁶J. A. Lane, S. J. Benson, D. Walter, and J. A. Kilner, *Solid State Ionics* **121**, 201 (1999).

⁷I. C. Fullarton, J. A. Kilner, B. C. H. Steele, and P. H. Middleton, *Proceedings of the Second International Symposium on Ionic and Mixed Conducting Ceramics*, edited by T. A. Ramanarayanan, W. L. Worrell, and H. L. Tuller (The Electrochemical So-

ciety, Pennington, NJ, 1994), p. 9.

⁸S. J. Benson, R. J. Chater, and J. A. Kilner, *Proceedings of the Third International Symposium on Ionic and Mixed Conducting Ceramics*, edited by T. A. Ramanarayanan (The Electrochemical Society, Pennington, NJ, 1997), p. 596

⁹D. J. Goossens, K. F. Wilson, M. James, A. J. Studer, and X. L. Wang, *Phys. Rev. B* **69**, 134411 (2004).

¹⁰W. Kobayashi, S. Ishiwata, I. Terasaki, M. Takano, I. Grigoraviciute, H. Yamauchi, and M. Karppinen, *Phys. Rev. B* **72**, 104408 (2005).

¹¹E. V. Antipov, A. M. Abakumov, and S. Ya. Istomin, *Inorg. Chem.* **47**, 8543 (2008).

¹²S. Kimura, Y. Maeda, T. Kashiwagi, H. Yamaguchi, M. Hagiwara, S. Yoshida, I. Terasaki, and K. Kindo, *Phys. Rev. B* **78**, 180403(R) (2008).

¹³S. Ya. Istomin, O. A. Drozhzhin, Ph. S. Napolosky, S. N. Putilin, A. A. Gippius, and E. V. Antipov, *Solid State Ionics* **179**, 1054 (2008).

- ¹⁴S. Ya. Istomin, J. Grins, G. Svensson, O. A. Drozhzhin, V. L. Kozhevnikov, E. V. Antipov, and J. P. Attfield, *Chem. Mater.* **15**, 4012 (2003).
- ¹⁵F. Lindberg, O. A. Drozhzhin, S. Ya. Istomin, G. Svensson, F. B. Kaynak, P. Svedlindh, P. Warnicke, A. Wannberg, A. Møllergaard, and E. V. Antipov, *J. Solid State Chem.* **179**, 1434 (2006).
- ¹⁶D. C. Parfitt, D. A. Keen, S. Hull, W. A. Crichton, M. Mezouar, M. Wilson, and P. A. Madden, *Phys. Rev. B* **72**, 054121 (2005).
- ¹⁷A. R. Cleave, J. A. Kilner, S. J. Skinner, S. T. Murphy, and R. W. Grimes, *Solid State Ionics* **179**, 823 (2008).
- ¹⁸A. Choneos, R. W. Grimes, B. P. Uberuaga, and H. Bracht, *Phys. Rev. B* **77**, 235208 (2008).
- ¹⁹M. Posselt, F. Gao, and H. Bracht, *Phys. Rev. B* **78**, 035208 (2008).
- ²⁰A. Choneos, H. Bracht, C. Jiang, B. P. Uberuaga, and R. W. Grimes, *Phys. Rev. B* **78**, 195201 (2008).
- ²¹A. Choneos, H. Bracht, R. W. Grimes, and B. P. Uberuaga, *Appl. Phys. Lett.* **92**, 172103 (2008).
- ²²M. Born and J. E. Mayer, *Z. Phys.* **75**, 1 (1932).
- ²³P. P. Ewald, *Ann. Phys.* **64**, 253 (1921).
- ²⁴R. A. Buckingham, *Proc. R. Soc. London, Ser. A* **168**, 264 (1938).
- ²⁵R. W. Grimes, D. J. Binks, and A. B. Lidiard, *Philos. Mag. A* **72**, 651 (1995).
- ²⁶M. A. McCoy, R. W. Grimes, and W. E. Lee, *Philos. Mag. A* **75**, 833 (1997).
- ²⁷R. W. Grimes, G. Busker, M. A. McCoy, A. Choneos, J. A. Kilner, and S. P. Chen, *Ber. Bunsenges. Phys. Chem.* **101**, 1204 (1997).
- ²⁸D. J. Binks, Ph.D. thesis, University of Surrey, 1994.
- ²⁹G. Busker, A. Choneos, R. W. Grimes, and I. W. Chen, *J. Am. Ceram. Soc.* **82**, 1553 (1999).
- ³⁰L. Minervini, R. W. Grimes, J. A. Kilner, and K. E. Sickafus, *J. Mater. Chem.* **10**, 2349 (2000).
- ³¹M. R. Levy, C. R. Stanek, A. Choneos, and R. W. Grimes, *Solid State Sci.* **9**, 588 (2007).
- ³²W. C. Swope, H. C. Andersen, P. H. Berens, and K. R. Wilson, *J. Chem. Phys.* **76**, 637 (1982).
- ³³W. Smith and T. R. Forester, *J. Mol. Graphics* **14**, 136 (1996).
- ³⁴W. Smith and I. Todorov. *The DLPOLY 3.0 User Manual*, Daresbury Laboratory, UK.
- ³⁵S. Nosé, *J. Chem. Phys.* **81**, 511 (1984).
- ³⁶W. G. Hoover, *Phys. Rev. A* **31**, 1695 (1985).
- ³⁷M. J. Gillan, *Physica B* **131**, 157 (1985).